Design and experimental assessment of an anti-windup for LTI state-constrained control of wave energy converters

Design and experimental assessment of an anti-windup for LTI state-constrained control of wave energy converters ⋆

Nicolás Faedo [*,1] **Francesco Ferri** [**] **Fabio Carapellese** [*]
Ted K. A. Brekken [***]

[*] *Marine Offshore Renewable Energy Lab., Dept. of Mechanical and Aerospace Engineering, Politecnico di Torino.*
[**] *Department of the Built Environment, Aalborg University.*
[***] *Electrical Engineering and Computer Science, Oregon State University.*

Abstract: Motivated by the necessity of suitable state constraint mechanisms within linear time-invariant (LTI) energy-maximising control of wave energy converters (WECs), this discussion paper presents an anti-windup (AW) scheme for *state* constraint satisfaction, where the associated unconstrained controller is designed via impedance-matching theory for WEC systems. As in the standard (input) AW scenario, the adopted technique provides a mechanism for 'informing' the (unconstrained) controller when constraints are active, so that appropriate modifications to future control actions can be taken accordingly. The overall adopted AW technique is tested experimentally, on a prototype of the Wavestar WEC system, available at Aalborg University (Denmark).

Keywords: Wave energy converters, Impedance-matching, Anti-windup, State constraints

1. MOTIVATION

In the light of the inherent requirement of effective state constraint handling mechanisms for wave energy conversion (WEC) systems (see *e.g.* (Faedo et al., 2020)), we present, in this discussion paper, an anti-windup (AW) scheme for state constraint satisfaction, where the associated (unconstrained) energy-maximising control is designed via linear impedance-matching theory. An AW setup is discussed, based on the structure proposed in (Rojas and Goodwin, 2002), which can be applied to a general class of non-optimisation-based WEC strategies. The AW scheme incorporates a tailored design for the associated limiting circuit, able to map the defined state constraints into an associated (time-varying) input constraint set. The combination between LTI energy-maximising controller and proposed AW technique, is tested experimentally, using a prototype of the Wavestar WEC system (Hansen and Kramer, 2011), available within the tank-testing facilities of Aalborg University, Denmark. We explicitly demonstrate that the proposed AW scheme is able to consistently respect the defined state constraints, having a mild impact on the overall energy absorption performance when compared to its unconstrained counterpart.

1.1 Notation

$\mathbb{R}^+$ and $\mathbb{C}^0$ are used to indicate the set of non-negative real numbers, and the set of complex numbers with zero real-part, respectively, while $\mathbb{C}_{<0}$ denotes the set of complex numbers with negative real-part. The Laplace transform of a function f, provided it exists, is denoted as $F(s)$, $s \in \mathbb{C}$. The Hermitian operator is denoted by $F(\jmath\omega)^\star$, with $\omega \in \mathbb{R}$. The saturation function is defined as $\text{sat}_\Delta(x) = \text{sign}(x)\min(|x|, \Delta)$, $\Delta \in \mathbb{R}^+$, and $x \in \mathbb{R}$. Finally, given a continuous-time signal $g(t)$, its discrete-time zero-order hold equivalent is denoted as $g[k]$.

2. EXPERIMENTAL WEC SYSTEM

The experimental system considered within this discussion paper, illustrated in Figure 1, is a small-scale (1:20) prototype of the Wavestar WEC device (Hansen and Kramer, 2011), tested within the basin facilities available at Aalborg University, Denmark, as part of a larger experimental campaign in WEC modelling and control, executed in September 2022. The system, which has been previously selected as a benchmark case for WEC control assessment within the first edition of the Wave Energy Control Competition (WEC^{3}OMP) (Ringwood et al., 2017), is essentially composed of a floater, connected through an arm to a pivoting point fixed at a reference frame. In equilibrium position, the arm sits at approximately 30° with respect to the horizontal reference frame. The system is free to move in a single degree-of-freedom, and extracts energy from pitch motion (about the reference point - see Figure 1) via the corresponding power take-off system (PTO, linear motor/generator) sitting on the upper structural joint of the device arm. Though we avoid a full description of each of the WEC components for economy of space, we refer the reader to (Ringwood et al., 2017) for further detail.

⋆ Nicolás Faedo has received funding from the European Union's Horizon 2020 research and innovation programme under the Marie Sklodowska-Curie grant agreement No 101024372.
[1] Corresponding author - e-mail: *nicolas.faedo@polito.it.*

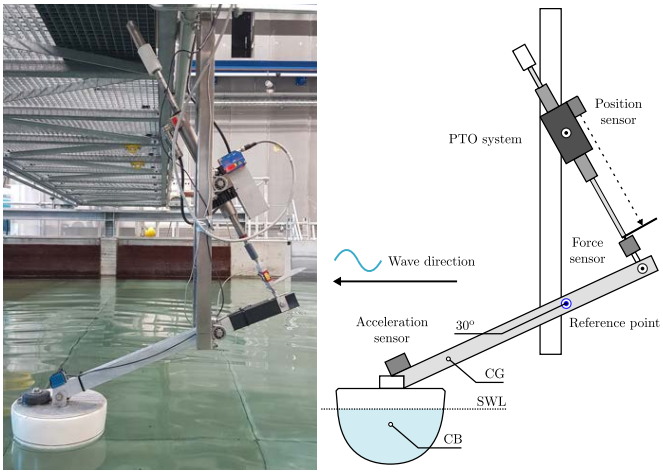

Fig. 1. Experimental prototype of the Wavestar system (left) and corresponding schematic (right).

3. ENERGY-MAXIMISING CONTROL DESIGN

Throughout this study, and adopting the arguments posed within the WEC^{3}OMP (Ringwood et al., 2017), we assume that the prototype WEC system, described in Section 2, can be modelled in terms of a representative linear map $G : \mathbb{C} \to \mathbb{C}, s \mapsto C(s\mathbb{I}_n - A)^{-1}B \in \mathcal{RH}_2$, defined in terms of a minimal state-space realisation as

$$G(s) \equiv \begin{cases} \dot{x}(t) = Ax(t) + B(d_\theta(t) + u_\theta(t)), \\ y_\theta(t) = Cx(t), \end{cases} \tag{1}$$

with $(A, B, C^\mathsf{T}) \in \mathbb{R}^{n\times n} \times \mathbb{R}^n \times \mathbb{R}^n$, and where $G(s)$ is of relative degree 1. Equation (1) characterises the input-output (I/O) relation

$$Y_\theta(s) = G(s)\left(D_\theta(s) + U_\theta(s)\right), \tag{2}$$

where y_θ is the device (pitch) velocity about the reference point (see Figure 1), d_θ is the (uncontrollable) wave excitation torque due to the action of the wave field, and u_θ is the control torque, supplied via the PTO system.

Following the requirement of energy-maximisation in WEC systems, and adopting a frequency-domain approach, the optimal control solution u_θ for maximum power transfer can be derived via the so-called impedance-matching principle (Faedo et al., 2022), where the WEC system is essentially described in terms of an *impedance*, analogously to standard circuit theory. Briefly summarising, let $I : \mathbb{C}^0 \to \mathbb{R}$, $\jmath\omega \mapsto I(\jmath\omega)$ be the *impedance* map of the prototype WEC system, defined as

$$I(\jmath\omega) = 1/G(\jmath\omega). \tag{3}$$

With the definition in (3), the (frequency-domain) optimal control solution (*load*), can be simply written as

$$U_\theta(\jmath\omega) = -I(\jmath\omega)^\star Y_\theta(\jmath\omega), \tag{4}$$

which is, in essence, an output feedback structure.

Remark 1. Though one can be tempted to use the analytic continuation of $I^\star$ to $\mathbb{C}$, in order to implement the control structure in (4), the resulting transfer function is inherently *non-causal*, due to the nature of the analytic continuation of the Hermitian operator (Scruggs, 2010).

Remark 1 refers to a well-known issue in design and synthesis of wave energy control systems. One can, although, approximate condition (4) by employing tailored causal and stable control structures, *i.e.* implementable. In particular, within this study, we consider a first-order biproper controller, defined as

$$K(s) = \alpha_1 s/(s + \alpha_2), \tag{5}$$

where the set of parameters $\mathscr{A} = \{\alpha_1, \alpha_2\}$ are uniquely computed as the solution of the interpolation equation

$$K(\jmath\omega_\mathcal{I}) = I(\jmath\omega_\mathcal{I})^\star, \tag{6}$$

with $\omega_\mathcal{I} \in \mathbb{R}^+$ a suitably selected interpolation frequency.

Remark 2. For the case of the prototype WEC system considered, the set $\mathscr{A} \subset \mathbb{R}^+$ (see also Section 5), and hence (5) is both stable and minimum-phase.

4. AW FOR STATE CONSTRAINT HANDLING

Within this section, we introduce the adopted AW scheme for state constraint satisfaction, tailored for the WEC prototype presented in Section 2, and the control structure defined in Section 3. Throughout this section, we consider the discrete-time equivalents $\{G_\mathrm{d}(q), K_\mathrm{d}(q)\}$ (with q the forward-shift operator) corresponding with the transfer functions $G(s)$ and $K(s)$ in equations (2) and (5), respectively, computed via a standard zero-order hold procedure with a sufficiently small sampling time $T_\mathrm{s} \in \mathbb{R}^+$. Furthermore, we write G_d in terms of a state-space realisation

$$G_\mathrm{d}(q) \equiv \begin{cases} x[k+1] = A_\mathrm{d}x[k] + B_\mathrm{d}\left(d_\theta[k] + u_\theta[k]\right), \\ y_\theta[k] = C_\mathrm{d}x[k], \end{cases} \tag{7}$$

where the triple of matrices $(A_\mathrm{d}, B_\mathrm{d}, C_\mathrm{d})$ stem directly from (1). We further assume that (7) is subject to a set of state constraints defined in terms of the velocity y_θ, *i.e.*

$$y_\theta[k] = C_\mathrm{d}x[k] \in \mathbb{Y} \triangleq [-\Delta, \Delta], \Delta \in \mathbb{R}^+. \tag{8}$$

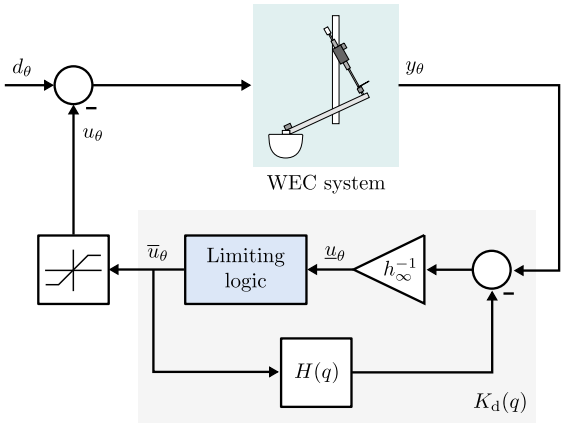

Fig. 2. General AW scheme for input constraints.

Figure 2 illustrates a general scheme for AW in the (standard) case of input constraints (see *e.g.* (Galeani et al., 2009)). In particular, following an analogous procedure to that in (Rojas and Goodwin, 2002), and given that the controller K_d is biproper, stable, and minimum-phase (see Remark 2), we can decompose its transfer function as

$$K_\mathrm{d}(q)^{-1} = h_\infty + H(q), \tag{9}$$

where h_∞ is the high frequency gain of $K_\mathrm{d}(q)^{-1}$, and $H(q)$ is both stable and strictly proper.

Focusing on the development of an AW scheme for the WEC state constraint case, we note that the set $\mathbb{Y}$ defines a corresponding input constraint set $\mathbb{U}$. The latter, although,

is inherently time-varying, as discussed in the following. Consider system (7) subject to the state constraint in (8). Since G_d is strictly proper with relative degree 1, a one-step ahead prediction of y_θ can be computed as

$$y_\theta[k+1] = C_\mathrm{d}A_\mathrm{d}x[k] + C_\mathrm{d}B_\mathrm{d}\left(d_\theta[k] + u_\theta[k]\right), \qquad (10)$$

where $\mathbb{R} \ni C_\mathrm{d}B_\mathrm{d} \neq 0$. Solving for u_θ in equation (10), we can define the following transition map $\Gamma : \mathbb{R}\times\mathbb{R}^n\times\mathbb{R} \to \mathbb{R}$

$$\Gamma(y_\theta, x, d_\theta) = \left(C_\mathrm{d}B_\mathrm{d}\right)^{-1}\left(y_\theta - C_\mathrm{d}A_\mathrm{d}x\right) - d_\theta. \qquad (11)$$

Note that the function Γ, as defined in (11), can be effectively used to map the state constraint set $\mathbb{Y}$ to an equivalent time-varying input constraint set $\mathbb{U}(x, d_\theta) = \Gamma(\mathbb{Y}, x, d_\theta)$. In particular, for a given value of y_θ, the induced input constraint set can be explicitly written as

$$\mathbb{U} \triangleq \left[\Delta^\mathrm{l}(x, d_\theta), \Delta^\mathrm{u}(x, d_\theta)\right] \subset \mathbb{R}, \qquad (12)$$

with

$$\begin{aligned}\Delta^\mathrm{l}(x, d_\theta) &= \left(C_\mathrm{d}B_\mathrm{d}\right)^{-1}\left(-\Delta - C_\mathrm{d}A_\mathrm{d}x\right) - d_\theta,\\ \Delta^\mathrm{u}(x, d_\theta) &= \left(C_\mathrm{d}B_\mathrm{d}\right)^{-1}\left(\ \ \Delta - C_\mathrm{d}A_\mathrm{d}x\right) - d_\theta,\end{aligned} \qquad (13)$$

where, clearly, it follows that $y_\theta \in \mathbb{Y} \Leftrightarrow u_\theta \in \mathbb{U}$, $\forall k \in \mathbb{N}$.

With the time-varying set derived in equation (13), an AW scheme, effectively able to handle the state constraint $\mathbb{Y}$ in (8), can be defined in terms of the limiting logic presented in Figure 3. In particular, the adopted AW is, in essence, a two-step procedure, which can be summarised as follows:

- Let $x[k]$ and $d_\theta[k]$ be the current state of system (7) and wave excitation input, respectively, and $\underline{u}_\theta[k]$ the control law required by the controller K_d. A one-step prediction $\hat{y}_\theta[k+1]$ can be computed via (10).
- Constraint violations in accordance with the set $\mathbb{Y}$ are subsequently detected in the prediction $\hat{y}$ by applying the saturation map $\mathrm{sat}_\Delta(\cdot)$. Based on the saturated value of $\hat{y}[k+1]$, an allowed control action $\overline{u}_\theta[k]$ can be back-calculated using the map $\Gamma(\cdot, x, d_\theta)$ in (11).

Remark 3. Clearly, if no constraint violation is detected, $\underline{u}_\theta = \overline{u}_\theta$, *i.e.* the unconstrained control solution, associated with the energy-maximising controller K_d, is directly applied to the WEC. If, on the contrary, the constraint on y_θ is active, $\overline{u}_\theta$ takes y_θ to the limit of the set $\mathbb{Y}$.

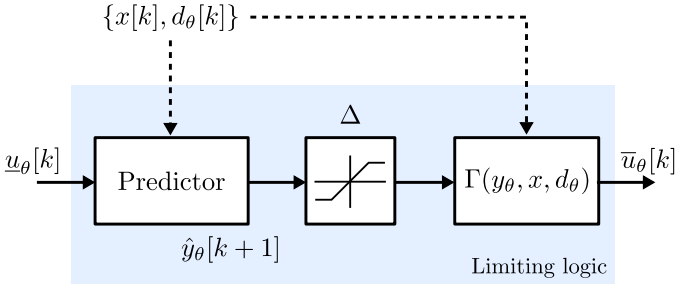

Fig. 3. Adopted AW limiting logic.

Remark 4. Effective implementation of the discussed AW structure requires instantaneous knowledge of the state-vector x and the wave excitation torque d_θ, in order to effectively back-calculate admissible control actions via (11). Such estimates can be computed in following standard unknown-input estimation techniques (Peña-Sanchez et al., 2019).

5. EXPERIMENTAL RESULTS

We present, in this section, an experimental assessment of the AW scheme detailed in Section 4, comprising the energy-maximising control design as in Section 3, and applied to the prototype described in Section 2. For performance assessment, we consider an irregular sea-state characterised in terms of a JONSWAP spectrum, with [2] a significant wave height $H_\mathrm{s} = 0.063$ [m], typical peak period $T_\mathrm{p} = 1.412$ [s], and enhancement factor $\gamma = 3.3$. The wave duration is set to 300 [s], which corresponds with more than 150 typical peak periods. The sampling time, considered both for data-acquisition, and corresponding discretisation of system/controller, is set to $T_\mathrm{s} = 0.005$ [s].

Within this study, the WEC model (1), characterising the behaviour of the experimental prototype, is obtained using black-box system identification procedures. To summarise, a set of down-chirp signals with different amplitudes (in the interval $[1, 4]$ [Nm]) is injected into the system as input (torque) signals, generating a corresponding set of output (velocity) responses. Each I/O pair is used to compute a frequency-domain empirical transfer function estimate (Ljung, 1998), and their corresponding average is used as target data-set for subspace-based identification techniques.

With respect to the energy-maximising controller $K(s)$, as defined in equation (5), the interpolation frequency $\omega_\mathcal{I}$ is chosen in terms of the energetic period associated with the sea-state considered, *i.e.* $\omega_\mathcal{I} = 2\pi/(0.9T_\mathrm{p})$ producing a corresponding set of parameters $\alpha_1 = 14.41$ and $\alpha_2 = 5.11$.

Concerning the specifics associated with the state AW scheme itself, the constraint set $\mathbb{Y}$, characterising the state limitation in (8), is set to $\Delta = 0.4$ [rad/s]. Note that this value is conservative for this device (and sea-state), and has been chosen to clearly illustrate the capabilities of the proposed state AW in experimental scenarios, under potentially severe constraint limits.

The results of applying the proposed AW scheme can be appreciated in Figure 4, where both the unconstrained (dotted), and constrained (solid), output response of the WEC are illustrated, together with each associated control input. Note that both responses are obtained in separate experiments using the same wave realisation, being the former only driven by the unconstrained controller $K(s)$, while the latter effectively incorporates the proposed AW, with all its components (*i.e.* energy-maximising controller, state/input observer, and associated constraint satisfaction logic). It can be straightforwardly seen that the AW technique is effectively able to enforce the imposed state constraint, being always within the limit considered, while the unconstrained controller consistently violates the maximum velocity value. Furthermore, note that, as expected from the arguments posed in Remark 3, the AW strategy provides an input correction *only* when the system is close to attain the constraint limit, by requiring an 'extra' torque to assist constraint satisfaction, yet being virtually the same as the unconstrained energy-maximising solution when the state constraint is not active.

Remark 5. Though small differences can be noted between unconstrained and constrained control solutions when the

[2] This sea-state corresponds with sea-state N°5 of the WEC^{3}OMP.

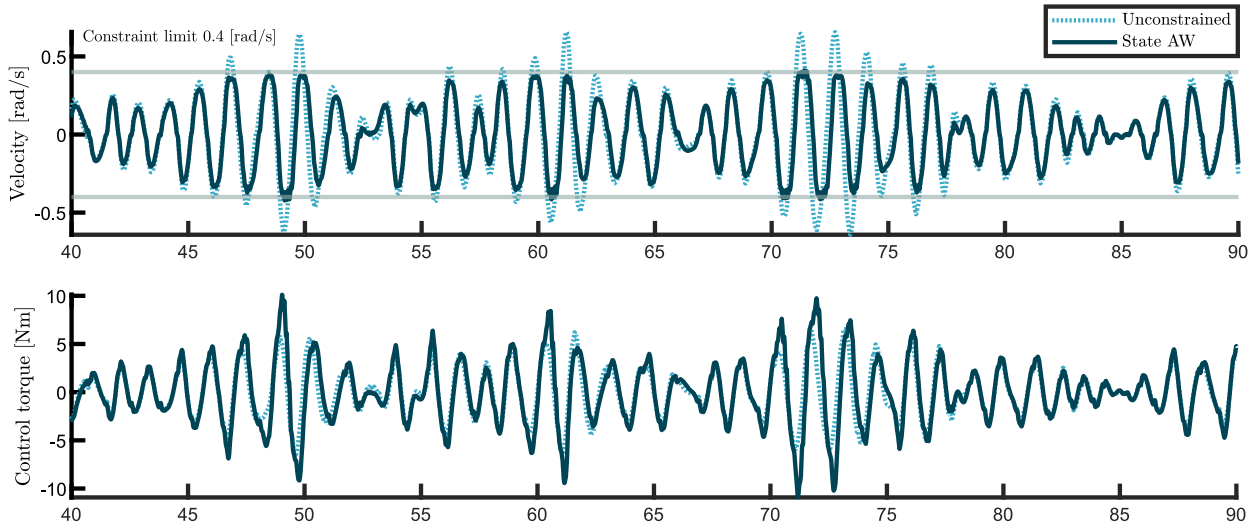

Fig. 4. Experimental WEC motion and associated control input for both unconstrained, and state-constrained AW case.

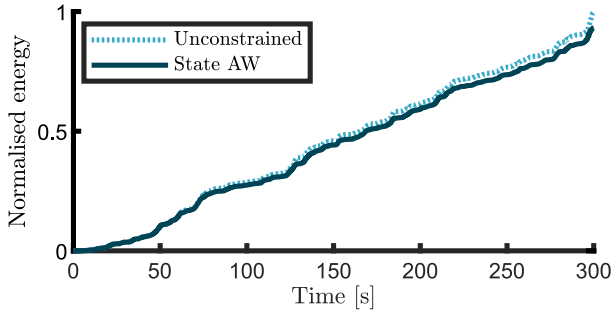

Fig. 5. Absorbed mechanical energy.

state constraint is inactive, these can be explained by the fact that both controllers are tested in separate experiments, where the same wave has to be realised by the associated wavemaker, which, although highly repetitive, presents slight differences in the effective wave generation.

Finally, Figure 5 presents an appraisal in terms of energy absorption, showing that the AW has a minimum influence on the overall loop performance, by virtue of the specific limitation logic, which modifies the unconstrained optimal solution only when strictly necessary.

6. CONCLUSIONS

We present, in this discussion paper, an AW scheme for state constraint handling in LTI energy-maximising control of WEC systems. The technique provides a mechanism for 'informing' the (unconstrained) controller when state constraints are active, so that appropriate modifications to future control actions can be taken accordingly. The combination between LTI energy-maximising controller and proposed AW technique, is tested experimentally, using a prototype of the Wavestar system. We demonstrate that the proposed AW scheme is able to consistently respect the defined state constraints, having a mild impact in the overall energy absorption performance. Future work will consider other LTI control structures for $K(s)$, including those of a broadbanded nature, reported in *e.g.* (García-Violini et al., 2020).

REFERENCES

Faedo, N., Carapellese, F., Pasta, E., and Mattiazzo, G. (2022). On the principle of impedance-matching for underactuated wave energy harvesting systems. *Applied Ocean Research*, 118, 102958.

Faedo, N., García-Violini, D., Peña-Sanchez, Y., and Ringwood, J.V. (2020). Optimisation-vs. non-optimisation-based energy-maximising control for wave energy converters: A case study. In *European Control Conference (ECC)*, 843–848.

Galeani, S., Tarbouriech, S., Turner, M., and Zaccarian, L. (2009). A tutorial on modern anti-windup design. In *2009 European Control Conference (ECC)*, 306–323.

García-Violini, D., Faedo, N., Jaramillo-Lopez, F., and Ringwood, J.V. (2020). Simple controllers for wave energy devices compared. *Journal of Marine Science and Engineering*, 8(10), 793.

Hansen, R.H. and Kramer, M.M. (2011). Modelling and control of the Wavestar prototype. In *Proceedings of the 9th European Wave and Tidal Energy Conference, EWTEC 2011*. University of Southampton.

Ljung, L. (1998). System identification. In *Signal analysis and prediction*, 163–173. Springer.

Peña-Sanchez, Y., Windt, C., Davidson, J., and Ringwood, J.V. (2019). A critical comparison of excitation force estimators for wave-energy devices. *IEEE Transactions on Control Systems Technology*, 28(6), 2263–2275.

Ringwood, J., Ferri, F., Ruehl, K.M., Yu, Y.H., Coe, R.G., Bacelli, G., Weber, J., and Kramer, M. (2017). A competition for WEC control systems. In *Proceedings of the 12th European Wave and Tidal Energy Conference 27th Aug-1st Sept 2017*, 831, 1–9. European Wave and Tidal Energy Conference 2017.

Rojas, O.J. and Goodwin, G.C. (2002). A simple anti-windup strategy for state constrained linear control. *IFAC Proceedings Volumes*, 35(1), 109–114.

Scruggs, J. (2010). On the causal power generation limit for a vibratory energy harvester in broadband stochastic response. *Journal of Intelligent Material Systems and Structures*, 21(13), 1249–1262.